J Adv Manuf Eng, Vol. 5, Issue. 2, pp. 47–60, December, 2024

Journal of Advances in Manufacturing Engineering
Web page info: https://jame.yildiz.edu.tr
DOI: 10.14744/ytu.jame.2024.00007

Original Article

A comprehensive statistical evaluation of shear and peel stresses in adhesively bonded joints

Bertan BEYLERGİL*

Department of Mechanical Engineering, Alanya Alaaddin Keykubat University Faculty of Engineering, Antalya, Türkiye

ARTICLE INFO

Article history
Received: 18 September 2024
Accepted: 17 October 2024

Key words:
Adhesively bonded joints, goland and reissner model, peel stress, polynomial regression, shear stress.

ABSTRACT

This study presents a detailed analysis of shear and peel stresses in adhesively bonded single lap joints using the Goland and Reissner analytical model. The investigation evaluates the effects of key parameters, including adhesive thickness, adhesive material, adherend material, and overlap length on stress distribution. A General Linear Model (GLM) and Analysis of Variance (ANOVA) are used to assess the significance of each factor. Results show that adhesive thickness contributes 36.55% to shear stress variation, followed by adhesive material (31.08%) and adherend material (25.83%). For peel stress, adhesive thickness accounts for 38.01% of the variation. A second-order polynomial regression model is employed to capture non-linear relationships between the input parameters and stress outcomes. The predicted shear stress of 8.676 MPa closely matches the actual value of 8.64 MPa, with a relative error of 0.42%, while the predicted peel stress of 10.9901 MPa aligns with the actual value of 11.04 MPa, with a relative error of 0.45%. The analysis highlights that thinner adhesive layers lead to higher stress concentrations, while thicker layers distribute stress more effectively. The choice of adhesive material and adherend material also significantly impacts stress levels. The study concludes that optimizing adhesive thickness, material selection, and overlap length is essential for improving the performance and reliability of adhesively bonded joints. The polynomial regression model successfully captures the non-linear stress behavior, offering a robust tool for predicting joint performance.

Cite this article as: Beylergil, B. (2024). A comprehensive statistical evaluation of shear and peel stresses in adhesively bonded joints. *J Adv Manuf Eng*, 5(2), 47–60.

INTRODUCTION

Adhesively bonded joints are widely used in various structural applications like aerospace, automotive, and civil engineering. These joints provide light weight and the possibility of joining dissimilar materials without damaging the structural integrity of the assembly [1]. Due to their increasing application, the complex interaction of various factors such as adhesive thickness, adherend material, and overlap length and environmental influences make the accurate prediction of their mechanical behavior under different loading conditions difficult to carry out [2].

Adhesive thickness is one of the major issues in the performance of ABJs. Several investigations demonstrated that optimum adhesive thickness is related to higher joint strength and reliability. Arenas et al. [3] considered 0.5 mm as the optimum value of adhesive thickness to obtain the maximum joint strength of structural joints. da Silva et al. [4] also identified adhesive thickness as one of the major factors contributing to a significant share of variance in shear strength, pointing out that smaller adhesive thicknesses minimize the concentration of stress, further adding to the general strength. Using the DOE approach, Lasprilla-Botero et al. [5] showed that adhesive formulations

*Corresponding author.
*E-mail address: bertan.beylergil@alanya.edu.tr

might be optimized in such a way as to result in improved performance, a fact that again reinforces the idea of proper thickness and material composition.

Similarly, Genty et al. [6] and Mishra et al. [7] showed that another more important factor influencing the joint performance was related to adhesive stiffness. In fact, stiffer adhesives increase the load-bearing capacity but also lead to higher stress concentrations. Zhao et al. [8] showed that the stiffness of the adhesive is a very important factor determining the pattern of the stresses in hybrid joints.

Geometric parameters, such as overlap length and joint configuration, have a significant impact on the performance of ABJs. da Silva et al. [9] and Vieira et al. [10] emphasized the importance of overlap length, showing that increasing overlap length reduces stress concentrations and improves joint strength. Zhang et al. [11] similarly showed that overlap length, along with joint geometry, influences the durability and load distribution in hybrid aluminum-CFRP joints. The studies consistently demonstrated that optimizing overlap length and adherend geometry can significantly enhance joint performance and reduce failure risk.

Studies by Haddou et al. [12] and Rangaswamy et al. [13] employed numerical and statistical models, such as Analysis of Variance (ANOVA) and DOE, to explore the effects of geometrical configurations. They found that overlap length, adhesive thickness, and adherend stiffness were the most significant factors affecting joint strength. Increasing overlap length by 20 mm, for example, resulted in a 25% increase in load-bearing capacity, while optimizing adhesive thickness further improved performance by reducing stress concentrations.

Failure modes in ABJs vary depending on adhesive thickness, geometry, and loading conditions. Choudhury and Debnath [14] reported a shift from adhesive failure to cohesive failure with thicker adhesive layers. Gajewski et al. [15] also observed cohesive failure at higher adhesive thicknesses, emphasizing the role of adhesive toughness in determining failure modes. Hybrid joints, combining adhesives with mechanical fasteners, have been shown to offer superior performance compared to purely bonded joints. Chen et al. [16] and Silva et al. [17] found that hybrid joints can withstand higher loads and absorb more energy during dynamic loading, significantly improving fatigue resistance.

Environmental factors, such as temperature, humidity, and exposure to harsh conditions, play a critical role in the long-term performance of ABJs. Bellini et al. [18] found that high temperatures and humidity significantly reduced joint strength, particularly for epoxy-based adhesives. Environmental effects were also studied by Gajewski et al. [15], who showed that exposure to moisture caused a 30% reduction in joint strength over time, particularly in high-humidity environments. Silva et al. [17] confirmed that joints subjected to elevated temperatures exhibited a shift in failure modes from cohesive to adhesive, further emphasizing the importance of environmental factors in joint design.

Tenreiro et al. [19] used damage metrics to detect voids and defects in bonded joints, which could compromise their performance in harsh environmental conditions. Their findings emphasized the need for continuous monitoring of ABJs in real-time applications, especially in aerospace and automotive industries, where environmental exposure can lead to premature failure.

Thanks to recent advances in statistical analysis and computational modeling, these factors have now been put under systematic analysis; therefore, more realistic predictions and better design optimization strategies can now be pursued. It focuses on some statistical techniques using ANOVA, GLM, and regression analysis for the analysis of recent research conducted in investigating some key parameters affecting shear and peel stresses in SLJs and machine learning. These methods help in the quantification of the effect of design parameters such as adhesive thickness, overlap length, and surface treatments with minimized experimental costs and provide certain suggestions on how different factors interact. One of the most widely used statistical approaches is the Taguchi method, which simplifies the optimization process by reducing the number of necessary experiments while maintaining statistical robustness. da Silva et al. [4] applied the Taguchi method to investigate the effect of adhesive thickness, overlap length, and adherend properties on the shear strength of single-lap joints, revealing that adhesive thickness accounted for 36.55% of the variance in joint strength. This method has proven valuable in complex engineering applications where multiple variables are involved, and it was successfully used by Rangaswamy et al. [13] to predict the strength of composite single-lap joints.

ANOVA is another essential statistical tool employed to analyze the effects of design parameters. For instance, Haddou et al. [12] used a factorial ANOVA to explore the interaction between adhesive thickness and overlap length, demonstrating that these factors have a significant impact on joint strength and stiffness. Their results showed that overlap length contributed 58.12% to the total variance in joint performance, while adhesive thickness accounted for 25.6%. ANOVA provides a detailed understanding of how different parameters contribute to the overall mechanical performance of joints, helping engineers to fine-tune their designs.

In addition to the Taguchi method and ANOVA, Response Surface Methodology (RSM) has been employed to model and optimize joint performance. Lasprilla-Botero et al. [5] utilized RSM to develop water-based adhesives for rubber-to-metal bonding, finding that factors such as resin content and curing time significantly impacted the mechanical properties of the adhesive. The use of RSM allowed them to construct predictive models with high accuracy, offering a comprehensive understanding of how formulation variables influence bond strength. Similarly, Mishra et al. [7] applied RSM to analyze the effects of adhesive modulus and geometric parameters on the free vibration frequency of adhesively bonded joints, demonstrating that optimized designs could improve joint stiffness and energy absorption.

The application of machine learning (ML) models, particularly artificial neural networks (ANNs), has gained popularity in recent years due to their ability to handle complex, non-linear relationships between design variables. Park et al. [20] utilized ANNs to predict the strength and failure modes of carbon fiber reinforced polymer SLJs, achieving

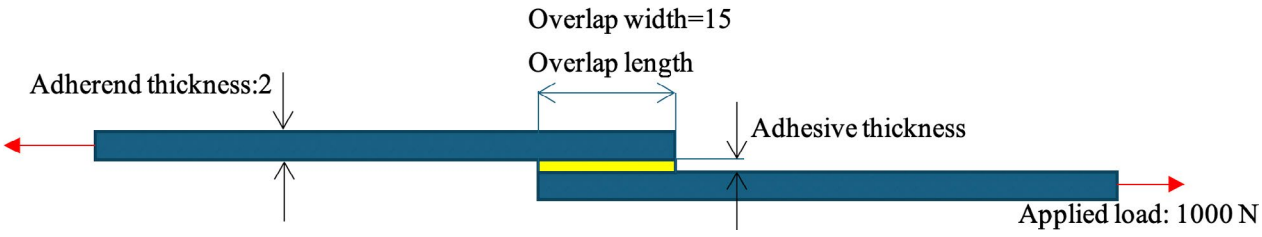

Joint parameters	Level 1	Level 2	Level 3
Adhesive thickness (mm)	0.15	0.25	0.35
Adhesive material	AV138	Araldite 2015	Hysol EA9321
Adherend material	Steel	Aluminum	Titanium
Overlap length (mm)	20	30	40

Figure 1. Configuration of adhesively bonded single lap joint with parameter levels (All dimensions in millimeters).

prediction accuracies exceeding 95%. The ANN model was able to capture the interactions between various parameters, such as surface treatments and bondline thickness, which traditional statistical models might struggle to quantify. Silva et al. [17] similarly employed ANNs to predict the fatigue life of hybrid joints, combining bonded and riveted components. Their results showed that the ANN models could accurately predict the number of cycles to failure, with a mean absolute percentage error (MAPE) of less than 3%. These findings highlight the capability of machine learning models to provide reliable predictions, even in the presence of highly complex and non-linear relationships.

Another key advantage of ANNs is their ability to learn from large datasets, making them particularly suited for high-throughput testing environments. Jensen et al. [21] demonstrated the effectiveness of ANNs in analyzing data from more than 1,200 single-lap joint specimens, optimizing the adhesive formulations and joint geometries. The model accurately predicted mechanical performance under varying load conditions and enabled the researchers to identify the most influential factors contributing to joint strength, such as adhesive modulus and bondline thickness.

In addition to ANNs, other machine learning algorithms, such as support vector machines (SVM) and decision trees, have been applied in the study of ABJs. Gajewski et al. [15] compared multiple machine learning techniques to predict the strength of adhesive joints subjected to uniaxial tensile testing. They found that SVMs and decision trees could provide reliable predictions, though ANNs outperformed them in terms of accuracy and computational efficiency. The study highlighted the potential of machine learning algorithms to support the optimization of ABJ designs, particularly in scenarios involving large datasets or complex parameter interactions.

Finally, probabilistic models combined with machine learning approaches have been used to assess the reliability of ABJs under uncertain conditions. For example, Zhao et al. [8] applied Monte Carlo simulations in conjunction with probabilistic models to evaluate the failure probability of hybrid joints under static and fatigue loading. The models accounted for uncertainties in material properties, joint geometry, and environmental factors, offering a more comprehensive approach to reliability analysis. Similarly, Mishra et al. [7] used probabilistic models to explore the effects of adhesive modulus and adherend properties on joint strength, demonstrating that a probabilistic approach could improve the reliability of joint designs, particularly in aerospace applications where safety is critical.

Previous studies have significantly advanced our understanding of the influence of adhesive thickness, adherend material, and overlap length on SLJ performance. However, this study provides a more comprehensive statistical analysis by integrating both linear and nonlinear models, including GLM and second-order polynomial regression. This approach enables a detailed examination of how adhesive thickness, material selection, and overlap length interact to affect shear and peel stresses, allowing for a more refined prediction of stress behavior, especially under complex loading conditions. To achieve this, the Goland and Reissner (GR) model, a foundational analytical approach widely recognized for its ability to account for eccentric load paths that generate bending moments and transverse forces, was employed influencing the stress state in these joints. The GR model strikes a balance between analytical simplicity and sufficient accuracy, making it a suitable choice for SLJs. Here, it is shown that the model's predictions closely align with both experimental data and more advanced analytical methods, validating its relevance for this study. By also incorporating a second-order polynomial regression model to capture non-linear stress behavior, a more nuanced understanding of joint performance is provided. This combined approach not only proven accuracy of the GR model but also enhances the analysis with a robust framework that optimizes joint performance, offering valuable insights into improving the design and reliability of SLJs in structural applications.

Problem Definition

This study focuses on the geometric configurations of adhesively bonded single lap joints in order to understand their interaction with shear and peel stress distribution. Figure 1 shows the single lap joint problem to be analyzed. The

Table 1. Mechanical properties (Quispe Rodríguez et al. [22], da Silva et al. [24])

Adherend	**Unit**	**Steel**	**Aluminum**	**Titanium**
Elastic modulus (*E*. GPa)	GPa	210	70	116
Poisson's ratio (*ν*.-)	–	0.3	0.3	0.34
Adhesive		**AV138**	**Araldite 2015**	**Hysol EA9321**
Elastic modulus (E_a)	GPa	4590	1850	3870
Shear modulus (G_a)	GPa	1.56	0.56	1.55
Poisson's ratio (*v*)	–	0.35	0.35	0.35

joints were configured with three different adhesive thicknesses, namely, 0.15 mm, 0.25 mm, and 0.35 mm, while using three adhesive materials Araldite 2015, AV138, and Hysol EA9321. The adherend materials will be Aluminum, Steel, and Titanium. Overlap lengths taken into consideration will be 20 mm, 30 mm, and 40 mm. An applied load taken for all configurations will be 1000 N. The specific levels for each parameter were chosen based on typical ranges encountered in practical applications. This work will explore the impact of adhesive thickness, material properties, and joint dimensions on the distribution of the bonded joint stress field.

GR Model

The GR model, developed in 1944, is a foundational analytical approach used to evaluate stress distributions in adhesively bonded single lap joints. This model is particularly significant because it considers the eccentric load path of the joint, which results in a bending moment and a transverse force at the ends of the overlap. These forces contribute to the overall stress state in the joint, leading to both shear and peel stresses in the adhesive layer.

The adhesive shear stress distribution τ found by Goland and Reissner is given by (Quispe Rodríguez et al. [22], Goland and Reissner [23]).

$$\tau = -\frac{1}{8}\frac{\bar{P}}{c}\left\{\frac{\beta c}{t}(1+3k)\frac{\cosh(\beta c/t)(x/c)}{\sinh(\beta c/t)}+3(1-k)\right\} \quad (1)$$

where $\bar{P}$ is the applied tensile load per unit width, c is the half of the overlap length, t is the adherend thickness, ν is the Poisson's ratio and k is the bending moment factor.

$$k = \frac{\cosh(u_2 c)}{\cosh\left(u_2 c + 2\sqrt{2}\sinh(u_2 c)\right)} \quad (2)$$

$$u_2 = \sqrt{\frac{3(1-\upsilon^2)}{2}}\frac{1}{t}\sqrt{\frac{\bar{P}}{tE}} \quad (3)$$

$$\beta^2 = 8\frac{G_a}{E}\frac{t}{t_a} \quad (4)$$

where G_a and t_a are the shear modulus and the thickness of the adhesive layer. The adhesive peel stress distribution σ is given by

$$\sigma = \frac{1}{\Delta}\frac{\bar{P}t}{c^2}[A+B] \quad (5)$$

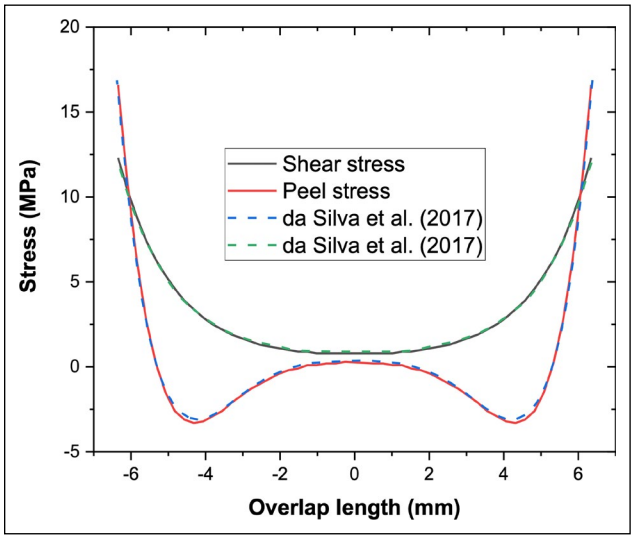

Figure 2. Comparison of the obtained shear and peel stresses with literature values.

where

$$A = \left(R_2\lambda^2\frac{k}{2}+\lambda k'\cosh(\lambda)\cosh(\lambda)\right)\cosh\left(\frac{\lambda x}{c}\right)\cos\left(\frac{\lambda x}{c}\right)$$
$$B = \left(R_1\lambda^2\frac{k}{2}+\lambda k'\sinh(\lambda)\sinh(\lambda)\right)\sinh\left(\frac{\lambda x}{c}\right)\sin\left(\frac{\lambda x}{c}\right) \quad (6)$$

$$k' = \frac{kc}{t}\sqrt{3(1-\nu^2)\frac{\bar{P}}{tE}} \text{ (the transverse force factor)} \quad (7)$$

$$\lambda = \gamma\frac{c}{t}, \gamma^4 = 6\frac{E_a}{E}\frac{t}{t_a}, \Delta = \frac{1}{2}(\sin(2\lambda)+\sinh(2\lambda)) \quad (8)$$

$$R_1 = \cosh(\lambda)\sinh(\lambda)+\sinh(\lambda)\cosh(\lambda)$$
$$R_2 = -\cosh(\lambda)\sinh(\lambda)+\sinh(\lambda)\cosh(\lambda) \quad (9)$$

where E and t are the elastic modulus and the thickness of the adherend material. Table 1 provides the material properties of the adherend and adhesive layer used for the calculations, serving as a basis for both the comparisons and analyses conducted in this work. The model equations were solved using the JointDesigner program. Material properties, geometric parameters, and applied loads were input into the program, which was used to compute the resulting stress distributions.

Table 2. Levels of adhesive thickness, adhesive material, adherend material, and overlap length with corresponding shear and peel stress values

Adhesive thickness (mm)	Adhesive material	Adherend material	Overlap length (mm)	Shear stress (MPa)	Peel stress (MPa)
1	1	1	1	13.92	18.91
1	1	1	2	13.13	17.42
1	1	1	3	12.46	16.16
1	1	3	1	18	24.22
1	1	3	2	16.77	21.88
1	1	3	3	15.76	19.98
1	1	2	1	22.17	29.44
1	1	2	2	20.4	26.06
1	1	2	3	19.02	23.44
1	2	1	1	9.04	12.11
1	2	1	2	8.48	11.16
1	2	1	3	8.04	10.35
1	2	3	1	11.64	15.53
1	2	3	2	10.82	14.03
1	2	3	3	10.17	12.82
1	2	2	1	14.32	18.9
1	2	2	2	13.16	16.74
1	2	2	3	12.26	15.06
1	3	2	3	17.5	21.57
2	1	2	3	14.85	18.27
2	2	2	3	9.61	11.75
2	3	1	3	8.96	11.57
2	3	3	3	11.34	14.32
2	3	2	3	13.68	16.81
3	1	1	3	8.28	10.67
3	1	3	3	10.47	13.2
3	1	2	3	12.63	15.51
3	2	1	1	6.28	7.99
3	2	1	2	5.72	7.38
3	2	1	3	5.39	6.84
3	2	3	1	7.88	10.28
3	2	3	2	7.26	9.29
3	2	3	3	6.81	8.49
3	2	2	1	9.62	12.54
3	2	2	2	8.82	11.1
3	2	2	3	8.21	9.99
3	3	1	1	8.6	11.48
3	3	1	2	8.05	10.58
3	3	1	3	7.63	9.81
3	3	3	1	11.05	14.73
3	3	3	2	10.27	13.31
3	3	3	3	9.65	12.15
3	3	2	1	13.59	17.93
3	3	2	2	12.49	15.87
3	3	2	3	11.64	14.28

For validation purposes, the study by da Silva et al. [24], which presented both the Goland and Reissner (GR) and Ojalvo and Eidinoff analytical solutions, was selected. These analytical solutions provided results that were very close to each other [24], demonstrating their consistency in predicting stress distributions. In this study, the aluminum adherend had a thickness of 1.62 mm, an overlap length of 12.7 mm, an adhesive thickness of 0.25 mm, and a width of 25.4 mm, with the adhesive having an elastic modulus of 4.82 GPa and a Poisson's ratio of 0.4. The applied load was 1 kN, and as shown in Figure 2, the comparison of the obtained shear and peel stresses indicates that the model results are in good agreement with the literature.

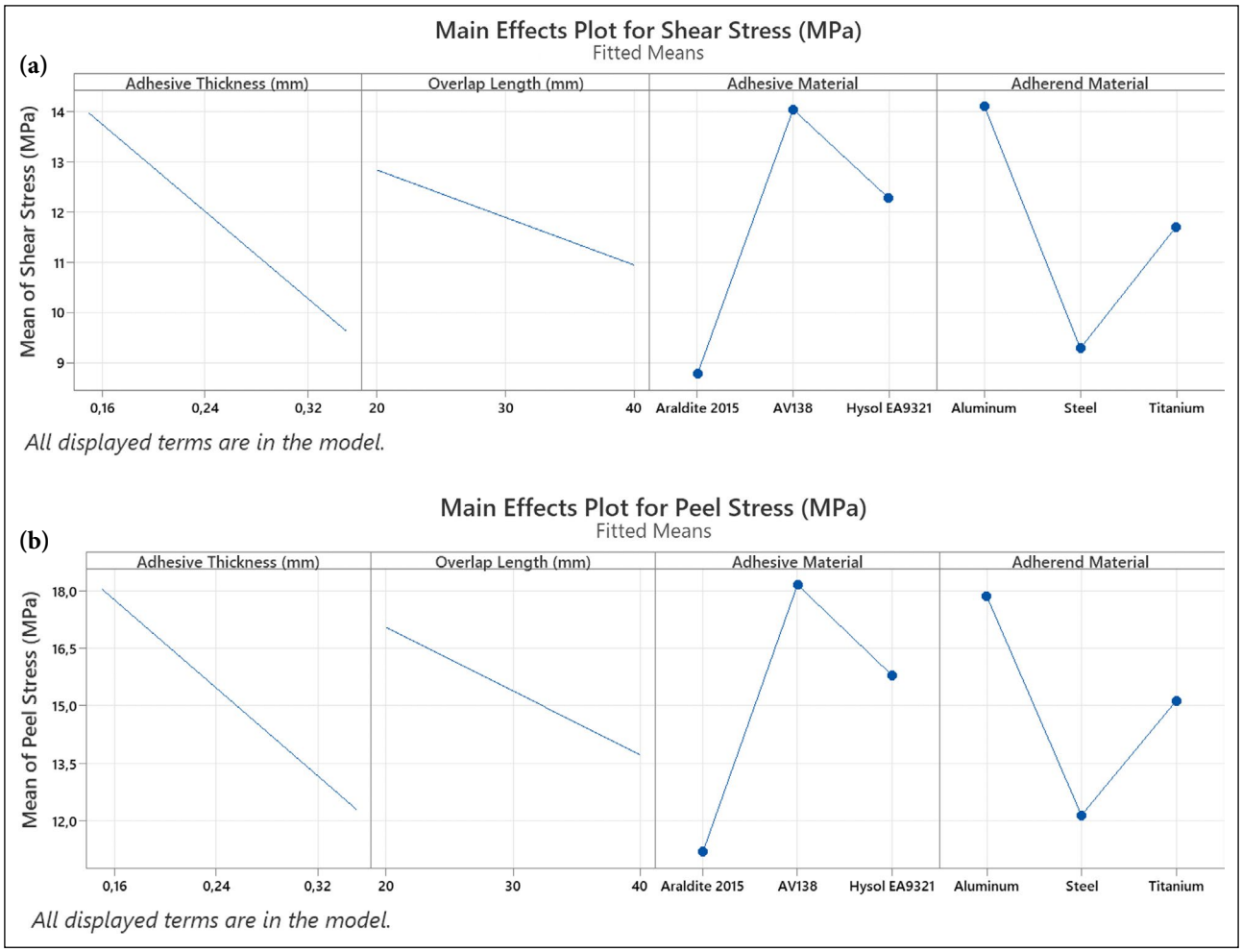

Figure 3. Main effect plot for **(a)** Shear and **(b)** Peel stress.

Dataset Creation Process

The dataset was developed by systematically exploring every possible combination of the selected parameters—adhesive thickness, adherend material, adhesive material, and overlap length. The objective was to capture the full spectrum of stress responses in adhesively bonded single lap joints. While the total number of possible configurations, based on the combination of all parameter levels, would be 81, the dataset includes only 45 data points. This suggests that certain combinations may have been unnecessary for the specific analysis, allowing the focus to remain on the most critical or feasible configurations. For each of these configurations, the Goland and Reissner analytical model was utilized to calculate the shear stress (τ) and peel stress (σ) values. Table 2 presents the different configurations of adhesive thickness, adherend material, adhesive material, and overlap length used in this analysis, structured to ensure that the most critical and feasible combinations of parameters were included. This approach allowed for an efficient exploration of the parameter space while maintaining a focus on the configurations most relevant to the study objectives.

RESULTS AND DISCUSSION

This section presents the detailed analysis of the effect of various parameters on shear and peel stresses in adhesively bonded single lap joints using Minitab software. The section proceeds with the main effects of parameters such as adhesive thickness, adhesive material, adherend material, and overlap length on shear and peel stresses. It then proceeds to explain the interaction effects where the interaction of the two aforementioned factors about stress behavior is elaborated through interaction plots.

After the interaction effects, the section develops a GLM analysis, presenting as a whole, the level of contribution by each parameter to the total variation in shear and peel stresses. The section now proceeds with discussions on second-order polynomial regression models in order to capture nonlinear relationships between input parameters and resulting stress outcomes. These models provide a more accurate prediction of the behavior of the stresses. In the section, both fitted line plots and actual versus predicted values of the stresses are included. Finally, in the same section, a comparison of the linear models is made against the polynomial ones, focusing on the strengths of the latter in describing the complexities of the stress distribution. After these, some practical implications are drawn by presenting some recommendations regarding design, based on the statistical analysis.

Main Effects of Parameters on Shear and Peel Stress

Figure 3a shows the main effects on shear stress. It is evident from the plot that adhesive thickness has a significant influence, with thinner adhesive layers (0.15 mm) resulting in

Table 3. ANOVA results

Source	DF	Seq SS	Contribution	Adj SS	Adj MS	F-value	P-value
Shear stress							
Adhesive thickness (mm)	2	248.86	36.55%	153.80	76.899	111.39	0.000
Adhesive material	2	211.65	31.08%	224.57	112.286	162.65	0.000
Adherend material	2	175.90	25.83%	179.45	89.724	129.96	0.000
Overlap length (mm)	2	19.70	2.89%	19.70	9.850	14.27	0.000
Error	36	24.85	3.65%	24.85	0.690		
Total	44	680.97	100.00%				
Peel stress							
Adhesive thickness (mm)	2	435.66	38.01%	267.28	133.639	112.06	0.000
Adhesive material	2	358.89	31.31%	391.12	195.560	163.98	0.000
Adherend material	2	244.91	21.37%	252.55	126.276	105.89	0.000
Overlap length (mm)	2	63.81	5.57%	63.81	31.907	26.75	0.000
Error	36	42.93	3.75%	42.93	1.193		
Total	44	1146.20	100.00%				

Table 4. Model summary

	S	R-sq	R-sq(adj)	Press	R-sq(pred)	AICc	BIC
Shear stress	0.830888	96.35%	95.54%	38.2309	94.39%	127.46	139.06
Peel stress	1.09204	96.25%	95.42%	66.0545	94.24%	152.06	163.65

higher shear stresses and thicker layers (0.35 mm) leading to reduced stress. This result aligns with expectations, as thinner adhesives tend to concentrate stresses at the bonded interface, whereas thicker adhesives better distribute the load. The effect of adhesive material is also notable, with AV138 leading to the highest shear stresses compared to Araldite 2015 and Hysol EA9321. The differences between these materials likely reflect their mechanical properties and ability to handle stresses. Regarding adherend material, aluminum results in the highest shear stress, followed by steel and titanium, indicating that the choice of adherend material significantly affects the stress distribution within the joint. Finally, overlap length also influences shear stress, but its effect is less pronounced compared to adhesive thickness or material. Longer overlap lengths, particularly 40 mm, reduce stress, while shorter lengths (20 mm) result in higher shear stresses.

Figure 3b shows a similar pattern for peel stress. Adhesive thickness again plays a key role, with thinner layers producing higher peel stresses. Thicker layers help distribute peel loads more evenly, reducing stress concentrations. The adhesive material has a similar ranking, with AV138 generating the highest peel stresses, followed by Hysol EA9321 and Araldite 2015. Aluminum once again leads to higher peel stress compared to steel and titanium, underscoring the importance of material properties in determining stress behavior. Overlap length has a relatively smaller effect on peel stress, but increasing the overlap length still contributes to a reduction in stress. Overall, the main effect plots confirm that adhesive thickness and material are the most influential factors for both shear and peel stress, while the effects of adherend material and overlap length are also important but somewhat less pronounced.

General Linear Model (GLM)

GLM analysis was conducted to evaluate the influence of adhesive thickness, adhesive material, adherend material, and overlap length on shear and peel stresses in adhesively bonded single lap joints. The statistical significance of each factor and its contribution to the total variation were determined through ANOVA. The results highlight the importance of each factor in determining the stress distributions.

Shear Stress Analysis

The ANOVA results for shear stress, presented in Table 3, demonstrate that adhesive thickness, adhesive material, adherend material, and overlap length all significantly influence the shear stress distribution. The adhesive thickness contributed 36.55% of the total variation, followed by the adhesive material (31.08%), and the adherend material (25.83%). Overlap length had the smallest impact, contributing only 2.89% to the total variation. All factors had p-values less than 0.05, indicating that they are statistically significant.

Additionally, the model summary (Table 4) confirms that the GLM explains 96.35% of the variance in shear stress, as indicated by the R-squared value. If the value of R^2 is high (close to 1), it suggests that the model has a good fit to the data, meaning the independent variables in the model explain a significant portion of the variability in the response. The adjusted R-squared value of 95.54% further supports the model's robustness in capturing the relationships between the input parameters and shear stress. The coefficients for each parameter in

Table 5. Coefficients

Term	Coef	SE coef	95% CI	T-value	P-value	VIF
Shear stress						
Constant	11.792	0.172	(11.443; 12.140)	68.61	0.000	
Adhesive thickness (mm)						
0.15	2.463	0.224	(2.008; 2.917)	10.98	0.000	2.91
0.25	-0.508	0.297	(-1.111; 0.095)	-1.71	0.096	2.60
Adhesive material						
Araldite 2015	-2.957	0.171	(-3.303; -2.610)	-17.31	0.000	1.32
AV138	2.285	0.202	(1.875; 2.694)	11.31	0.000	1.54
Adherend material						
Aluminum	2.448	0.173	(2.097; 2.798)	14.16	0.000	1.33
Steel	-2.435	0.179	(-2.798; -2.071)	-13.58	0.000	1.30
Overlap length (mm)						
20	0.869	0.192	(0.479; 1.259)	4.52	0.000	1.67
30	-0.026	0.192	(-0.416; 0.364)	-0.13	0.895	1.67
Peel stress						
Constant	15.245	0.226	(14.787; 15.703)	67.49	0.000	
Adhesive thickness (mm)						
0.15	3.251	0.295	(2.653; 3.849)	11.03	0.000	2.91
0.25	-0.678	0.391	(-1.471; 0.114)	-1.74	0.091	2.60
Adhesive material						
Araldite 2015	-3.899	0.225	(-4.355; -3.444)	-17.37	0.000	1.32
AV138	3.025	0.265	(2.486; 3.563)	11.40	0.000	1.54
Adherend material						
Aluminum	2.869	0.227	(2.408; 3.330)	12.63	0.000	1.33
Steel	-2.927	0.236	(-3.405; -2.450)	-12.43	0.000	1.30
Overlap length (mm)						
20	1.562	0.253	(1.049; 2.075)	6.18	0.000	1.67
30	-0.041	0.253	(-0.554; 0.471)	-0.16	0.871	1.67

Table 5 suggest that thinner adhesives (0.15 mm) lead to significantly higher shear stresses compared to thicker adhesives (0.35 mm). The choice of adhesive material also affects stress levels, with AV138 resulting in the highest shear stresses and Araldite 2015 the lowest due to the higher stiffness. Similarly, aluminum adherends generate higher shear stresses than steel or titanium, reinforcing the critical role of material properties.

Peel Stress Analysis

For peel stress, the results of the ANOVA also show very similar patterns to shear stress; the largest contribution comes from adhesive thickness, 38.01%, while adhesive material and adherend material came in at 31.31% and 21.37%, respectively. Overlap length again has a small but statistically significant effect, contributing 5.57% to the variation in peel stress. These findings are consistent with expectations given the key role that adhesive and adherent materials are expected to play in managing peel stress.

The R-square value in the model summary (Table 4) for peel stress is 96.25%, which shows that the developed GLM explains the variation in peel stress reasonably well. This can be seen from the adjusted R-square of 95.42%, which would account for the model's reliability to capture the effect of the input factors. Coefficients from Table 5 for the peel stresses follow the same pattern obtained from the shear stresses-the thinnest adhesives at 0.15 mm provide the highest peel stresses. AV138 once again produces the most intense peel stresses, and with aluminum as an adherend material creates a higher peel stress compared to steel or titanium.

Interaction Effects

Figures 4a and 4b present interaction plots that explore the effects of different adhesive materials (Araldite 2015, AV138, and Hysol EA9321) and adherend materials (Aluminum, Steel, and Titanium) on both shear stress and peel stress performance. Together, these figures provide valuable insights into the mechanical behavior of adhesive-adherend combinations, highlighting the significance of material selection in optimizing both shear and peel stress properties.

In Figure 4a, the relationship between adhesive-adherend combinations and shear stress reveals that AV138 consistently offers the highest mean shear stress values across all adherend materials, particularly with aluminum. This trend suggests

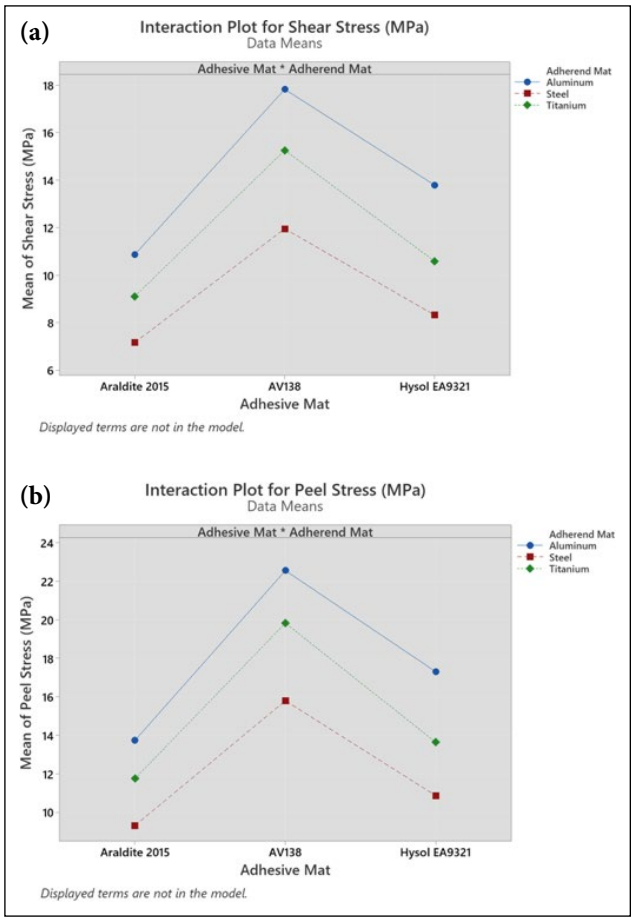

Figure 4. Interaction plot for **(a)** shear and **(b)** peel stress.

that AV138 is highly effective at resisting shear stress, especially when paired with aluminum. Araldite 2015 and Hysol EA9321 exhibit lower shear stress values, with Araldite 2015 generally outperforming Hysol EA9321 across all adherends. Among the adherend materials, aluminum consistently provides the best performance in shear stress, while steel, especially in combination with Hysol EA9321, shows the weakest performance, indicating that this pairing may not be suitable for applications requiring high shear resistance.

Similarly, Figure 4b explores the interaction between adhesive-adherend combinations and peel stress, which is closely related to the thickness of the adhesive. Again, AV138 demonstrates superior performance across all adherend materials, with a significant peak when used with aluminum. This trend mirrors the behavior observed in the shear stress plot, reinforcing the versatility and strength of AV138 as an adhesive. Araldite 2015 and Hysol EA9321 show lower peel stress values, with Araldite 2015 maintaining a slight advantage. Steel once again exhibits the lowest peel stress values, particularly when paired with Hysol EA9321, highlighting its weaker resistance to peel stress in this configuration. When comparing the results from both figures, it becomes clear that the adhesive AV138 consistently outperforms the other adhesives in terms of both shear and peel stress, particularly when used with aluminum. This adhesive-adherend combination is highly effective for applications where both high shear and peel stress resistance are required. In contrast, steel, especially when combined with Hysol EA9321, shows consistently poor performance across both stress types, making it the least favorable combination for structural applications demanding high mechanical integrity. The non-parallel lines further emphasize the significant interaction effects between adhesive and adherend materials. The performance of each adhesive is not constant but is heavily dependent on the type of adherend material used. For instance, while AV138 excels with aluminum, its advantage diminishes when used with steel or titanium. Similarly, the differences between Araldite 2015 and Hysol EA9321 are more pronounced with aluminum but less so with steel or titanium. This reinforces the importance of selecting the appropriate adhesive-adherend pair based on the specific stress conditions a structure is expected to endure.

Table 6. Model summary for polynomial regression of shear and peel stress

	S	R-sq	R-sq(adj)
Shear stress	0.733028	97.95%	97.85%
Peel stress	0.513232	98.99%	98.95%

In conclusion, the comparative analysis of Figures 4a and 4b highlights the critical role of adhesive-adherend interactions in determining the mechanical performance of bonded joints. The superior performance of AV138, particularly with aluminum, suggests it as the optimal choice for applications requiring high resistance to both shear and peel stress. Conversely, the combination of Hysol EA9321 with steel consistently shows poor performance, emphasizing the need for careful selection of materials in engineering applications to ensure the desired mechanical properties are achieved.

Polynomial Regression Analysis

In this section, the second-order polynomial regression analysis is performed, which can capture non-linear relationships between input variables with regard to adhesive thickness, material of adhesive, adherend material, and overlap length. Polynomial regression finds many applications in nonlinearities occurring in data, hence making more accurate predictions of the behavior of adhesively bonded joints.

Shear Stress Polynomial Regression

The polynomial regression model for shear stress incorporates both linear and quadratic terms, as shown in the following regression equation:

$$Predicted\ shear\ stress = -6.095 + 2.369(Shear\ Stress) - 0.04337(Shear\ Stress)^2 \quad (10)$$

In this model, the linear term with a coefficient of 2.369 shows that there is a positive dependence of input factors on shear stress. On the other hand, the negative quadratic term (-0.04337) shows that while shear stress increases at the beginning, it eventually levels off or decreases. This is a common phenomenon in most mechanical systems, where beyond certain values of load or input, material stress response reaches a diminishing return. The results of the regression analysis statistic can be seen in Table 6.

Table 7. Analysis of variance for polynomial regression of shear and peel stress

Source	DF	SS	MS	F	P
Shear stress					
Regression	2	1077.08	538.541	1002.25	0.000
Error	42	22.57	0.537		
Total	44	1099.65			
Peel stress					
Regression	2	1088.59	544.294	2066.36	0.000
Error	42	11.06	0.263		
Total	44	1099.65			

As shown in Table 7, the F-statistic of regression is very high (F=1002.25, p<0.000), and thus fits the data with statistical significance. Besides, an R-square value of 97.95% and adjusted R-squared of 97.85% also prove that this model explains almost all the variability in shear stress. This improvement in the goodness of fit, with respect to the linear model, suggests that the quadratic term has allowed the model to capture further complexities in the data.

Peel Stress Polynomial Regression

Similarly, the polynomial regression equation for peel stress includes both linear and quadratic terms:

$$\textit{Predicted peel stress} = -6.126 + 1.851(\textit{Peel Stress}) - 0.02644(\textit{Peel Stress})^2 \quad (11)$$

The positive linear term of 1.851 is directly proportional to the input factors and infers a positive relationship between these input factors and the output variable, peel stress. However, the negative quadratic term of -0.02644 introduces some negative curvature due to the possible non-linear relationship where the maximum value of peel stress increases up to a certain value and after that it decreases. Such behavior has been observed in bonded joints where the peel stresses are usually maximum at particular conditions and decrease beyond any critical load/thickness.

Table 7 presents the results of the variance analysis of the polynomial regression model fitted to peel stress. The F-statistic of the regression is even higher in the case of shear stress (F=2066.36, p<0.000), showing an extremely good fit to the data. With an R-squared of 98.99% and adjusted R-squared at 98.95%, this model captures almost all the variability in peel stress. This ascertains that the quadratic model captured the non-linearities effectively.

Sequential Analysis of Variance for Shear and Peel Stress

A detailed sequential ANOVA was done to check the contribution of both linear and quadratic terms for shear and peel stress models. Results are summarized in Table 8 and stated that both linear and quadratic terms contribute significantly to the level of stress in both the models. The linear term, in both cases, is the highest contributor to the variance: for the shear stress, F=866.78, and for the peel stress, F=1015.81, both with p=0.000, while the quadratic terms develop the models further to catch the non-linearities present in the data: F=54.73 for shear stress and F=127.54 for peel stress.

Table 8. Sequential analysis of variance for shear and peel stress

Source	DF	SS	F	P
Shear stress				
Linear	1	1047.68	866.78	0.000
Quadratic	1	29.41	54.73	0.000
Peel stress				
Linear	1	1054.99	1015.81	0.000
Quadratic	1	33.60	127.54	0.000

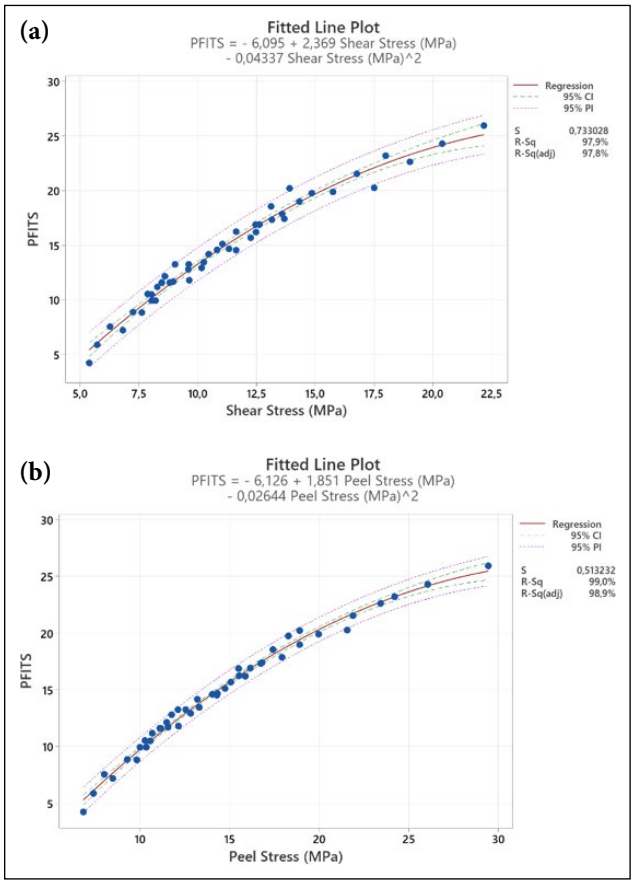

Figure 5. Fitted line plots for **(a)** shear and **(b)** peel stress.

Interpretation and Visual Representation

Figure 5 confirms the above conclusions from the polynomial regression analysis through fitted line plots for both shear and peel stresses. The fitted line in Figure 5a for the shear stress increases at first with the increase in input factors, but it quickly plateaus with further increases. As noted above, this is expected since the inclusion of the quadratic term in the model introduces negative curvature that limits the increase in shear stress to a saturation value. Similarly, Figure 5b shows the trend of peel stress that initially increases and then, due to the non-linear relation represented by the quadratic term, it reduces. Figure 5 emphasizes the need to consider nonlinear behavior in bonded joints. Plots of this nature demonstrate that while increasing adhesive thickness or overlap length can reduce stresses to a certain extent, further increases may not be proportionately helpful and may also lead to material failure due to large deformations.

Table 9. Variables used for the predictions

Variable	Setting
Case-1	
Adhesive thickness (mm)	0.4
Overlap length (mm)	25
Adhesive material	Araldite 2015
Adherend material	Aluminum
Case-2	
Variable	Setting
Adhesive thickness (mm)	0.5
Overlap length (mm)	30
Adhesive material	AV138
Adherend material	Titanium
Case-3	
Variable	Setting
Adhesive thickness (mm)	0.15
Overlap length (mm)	20
Adhesive material	Hysol EA9321
Adherend material	Steel

Comparison with Linear Models

These polynomial regression models should, therefore, be evaluated against the performance of the linear models discussed previously. The linear models allow one to get a good first approximation of the relation between input factors and stress outcomes. At the same time, the polynomial models can provide a more nuanced understanding because they can consider nonlinear behavior in their models. This is manifested in the higher R-squared values from polynomial models of 97.95% for shear stress and 98.99% for peel stress, compared to linear models with 96.35% for shear stress and 96.25% for peel stress.

Second-order polynomial terms also describe the "saturation" phenomenon, where beyond a certain value, increasing input variables results in less-than-proportional increases in output. In adhesive bonding joints, this translates to an optimum range within which adhesive thickness, material, and overlap length will provide a bond unhindered by too much of these parameters.

Predictions

The results of the prediction analysis for shear and peel stress are presented in this section. These predictions are made using the polynomial regression models derived earlier in the study. These have now been applied to certain sets of input parameters in order to see how well the predicted stress values match the analytical solutions obtained using the Goland and Reissner model. The objective of this analysis is to confirm that the regression models would be reliable in predicting the performance of adhesively bonded joints over the wide range of conditions.

The input variables used for the predictions are summarized in Table 9. These variables include adhesive thickness, overlap length, adhesive material, and adherend material. Three cases are considered to cover different joint configurations with varying material properties and geometrical parameters.

Table 10 presents the comparison for the three cases. In all cases, the predicted shear stress values closely match the analytical solutions, indicating a high degree of accuracy in the models.

- In Case 1, the predicted shear stress is 8.676 MPa, while the analytical solution is 8.64 MPa, resulting in a relative error of approximately 0.42%.
- In Case 2, the predicted shear stress is 8.898 MPa, compared to the analytical value of 9.41 MPa, with a relative error of 0.54%.
- In Case 3, the predicted shear stress is 13.258 MPa, closely matching the analytical solution of 12.82 MPa, with a relative error of 0.34%.

A similar comparison was performed for peel stress, as shown in Table 10. In all cases, the predicted peel stress values closely match the analytical solutions:

- In Case 1, the predicted peel stress is 10.9901 MPa, while the analytical value is 11.04 MPa, with a relative error of approximately 0.45%.
- In Case 2, the predicted peel stress is 11.525 MPa, compared to the analytical value of 12.15 MPa, with a relative error of 0.51%.
- In Case 3, the predicted peel stress is 17.865 MPa, closely aligning with the analytical value of 17.39 MPa, resulting in a relative error of 0.47%.

The close match between the predicted and analytical peel stress values further confirms the reliability of the

Table 10. Comparison of the predicted and analytical solutions

	Fit	Analytical	SE fit	95% CI	95% PI
Case-1					
Shear stress	8.67603	8.64	0.358363	(7.95056; 9.40150)	(6.82506; 10.5270)
Peel stress	10.9901	11.04	0.471519	(10.0356; 11.9446)	(8.55467; 13.4255)
Case-2					
Shear stress	8.89773	9.41	0.530962	(7.82285; 9.97260)	(6.88398; 10.9115)
Peel stress	11.5249	12.15	0.698618	(10.1106; 12.9392)	(8.57528; 14.1745)
Case-3					
Shear stress	13.2582	12.82	0.425676	(12.3964; 14.1199)	(11.3497; 15.1667)
Peel stress	17.8645	17.39	0.560087	(16.7306; 18.9983)	(15.3533; 20.3756)

polynomial regression models. The small errors in each case demonstrate that the models are capable of accurately estimating stress behavior in various joint configurations, providing a robust tool for predicting performance.

Practical Implications of Polynomial Regression

The polynomial regression models bear immense practical implication for design and optimization in adhesively bonded joints, thus enabling further insight into the nonlinear interactions of main parameters such as adhesive thickness, material properties, and overlap length. These models provide valuable insight into how these factors can be adjusted to optimize mechanical performance in joints under both shear and peel stress conditions.

One critical finding is the relationship between adhesive thickness and stress concentration. The models demonstrate that very thin adhesive layers (0.15 mm) result in high stress concentrations, which can lead to premature failure under loading. However, increasing the adhesive thickness to 0.35 mm significantly reduces both shear and peel stresses, distributing the load more evenly across the bonded area. Beyond this optimal thickness, further increases in adhesive thickness do not offer additional improvements and may, in fact, lead to joint failure due to excessive deformation and reduced structural integrity. This underscores the importance of carefully controlling adhesive layer thickness to balance stress distribution and avoid over-deformation of the joint.

Another significant factor that influences joint behavior is the choice of the adhesive material. While AV138 introduces higher stresses than Araldite 2015, it might provide better durability and resistance to fatigue in applications under cyclic loading. On the other hand, Araldite 2015 diminishes the level of stress concentrations and can possibly prolong the beginning performance of the joint, but it is more likely to fail during long cyclic conditions. These models provide a framework for such trade-offs to be assessed, and allow the engineer to choose the most appropriate adhesive for given operational requirements, balancing immediate stress management with long-term durability.

From the perspective of overlap length, the models indicate that beyond lengths of 30 mm, the return in terms of reduction in level of stress diminishes. Extension to 40 mm further improves the stress concentrations; the rate of improvement diminishes. Hence, an optimal overlap length of about 30 mm strikes the best balance between the ability of the joint to distribute stress and efficient material usage to minimize unnecessary weight and material cost while maintaining joint integrity.

These polynomial regression models are, in fact, robust tools to lead the design of adhesively bonded joints and provide engineers with actionable insight into how best to optimize adhesive thickness, material choice, and overlap length. The nonlinear relationship provided by the models helps them in making educated decisions to improve the performance of the joint and decrease the possibility of failure. This ensures that adhesively bonded joints can be designed in such a way that their demands are met in extreme high-stress environments and even long-term resistance to fatigue in application.

CONCLUSION

In this study, a detailed analysis of shear and peel stresses in adhesively bonded single lap joints using the Goland and Reissner model was conducted. The findings revealed that adhesive thickness is the most influential factor in stress distribution, followed closely by adhesive and adherend materials. The analysis highlighted that thinner adhesive layers lead to higher stress concentrations, whereas thicker layers help in distributing the stress more evenly, resulting in improved joint performance. A second-order polynomial regression model was employed to accurately capture the non-linear relationships between input parameters and stress outcomes, demonstrating the robustness of this approach in predicting joint behavior. The model's predictions showed high accuracy with minimal relative error, reinforcing the validity of the analytical methods used. However, it is essential to acknowledge the limitations of the Goland and Reissner model, particularly its assumptions and simplifications in addressing complex stress distributions. The model, while effective for initial analyses, may not capture the full range of mechanical behaviors in more intricate joint configurations. Therefore, future studies should aim to explore advanced analytical models or consider experimental validation to address these simplifications and provide a more comprehensive understanding of the stress behavior in adhesive joints.

Future Research

Future research could explore to use more advanced models that take into account the effects not modeled by the Goland and Reissner model. Such models will give even better representations of the true behavior for adhesively bonded joints and may present a view closer to reality for the real stress distributions. The experimental investigations to confirm the analytical predictions would be important for further refinement in the accuracy of the models. Physical tests on adhesively bonded joints, under various loading conditions, can be performed to extract information on the mechanical responses of the joint and identify discrepancies with theoretical models for enhancement of the general understanding of the joint behavior. The integration of finite element simulations with the analytical approach can enhance the calculation of the distribution of stresses in joints with complex geometries and/or loading conditions. FEA could be applied as a way to cross-validate the results obtained from the analytical models and would serve to give a far more detailed view of stress concentrations, therefore offering insight into potential areas of failure. New adhesives formulations and their interaction with the distribution of stress in bonded joints may, then, offer significant improvements in performances. The toughening of adhesives with additives or nanomaterials can be researched for interaction on the following: stress behavior, durability, failure modes, and development into more robust joint designs.

Acknowledgements

The author gratefully acknowledge financial support from the Scientific and Technological Research Council of Turkey (TÜBİTAK) with project number 218M710.

Data Availability Statement

The authors confirm that the data that supports the findings of this study are available within the article. Raw data that support the finding of this study are available from the corresponding author, upon reasonable request.

Conflict of Interest

The author declared no potential conflicts of interest with respect to the research, authorship, and/or publication of this article.

Use of AI for Writing Assistance

Not declared.

Ethics

There are no ethical issues with the publication of this manuscript.

REFERENCES

[1] Yildirim, C., Ulus, H., Beylergil, B., Al-Nadhari, A., Topal, S., & Yildiz, M. (2023). Effect of atmospheric plasma treatment on Mode-I and Mode-II fracture toughness properties of adhesively bonded carbon fiber/PEKK composite joints. *Engineering Fracture Mechanics, 289*, Article 109463. [CrossRef]

[2] Topal, S., Al-Nadhari, A., Yildirim, C., Beylergil, B., Kan, C., Unal, S., & Yildiz, M. (2023). Multiscale nano-integration in the scarf-bonded patches for enhancing the performance of the repaired secondary load-bearing aircraft composite structures. *Carbon, 204*, 112–125. [CrossRef]

[3] Arenas, J. M., Narbón, J. J., & Alía, C. (2010). Optimum adhesive thickness in structural adhesive joints using statistical techniques based on Weibull distribution. *International Journal of Adhesion and Adhesives, 30*(2), 160–165. [CrossRef]

[4] da Silva, L. F. M., Critchlow, G. W., & Figueiredo, M. A. V. (2008). Parametric study of adhesively bonded single lap joints by the Taguchi method. Journal of Adhesion *Science and Technology, 22*(13), 1477–1494. [CrossRef]

[5] Lasprilla-Botero, J., Álvarez-Láinez, M., Acosta, D. A., & Martín-Martínez, J. M. (2017). Water-based adhesive formulations for rubber to metal bonding developed by statistical design of experiments. *International Journal of Adhesion and Adhesives, 73*, 58–65. [CrossRef]

[6] Genty, S., Sauvage, J. B., Tingaut, P., & Aufray, M. (2017). Experimental and statistical study of three adherence tests for an epoxy-amine/aluminum alloy system: Pull-Off, Single Lap Joint, and Three-Point Bending tests. *International Journal of Adhesion and Adhesives, 79*, 50–58. [CrossRef]

[7] Mishra, P. K., Padhee, N., Panda, S. K., Kumar, E. K., & Panda, S. K. (2024). Free vibration frequency prediction to design optimum adhesively bonded composite double lap joint. *Journal of Vibration Engineering & Technologies, 12*, 5571–5584.

[8] Zhao, L., Shan, M., Liu, F., & Zhang, J. (2017). A probabilistic model for strength analysis of composite double-lap single-bolt joints. *Composite Structures, 161*, 419–427.[CrossRef]

[9] da Silva, L. F. M., Carbas, R. J. C., Critchlow, G. W., Figueiredo, M. A. V., & Brown, K. (2009). Effect of material, geometry, surface treatment and environment on the shear strength of single lap joints. *International Journal of Adhesion and Adhesives, 29*(6), 621–632. [CrossRef]

[10] Vieira, A. J. A., Campilho, R. D. S. G., & Madani, K. (2024). Statistical analysis of adhesive rod-tube joints under tensile stress for structural applications. *Journal of the Brazilian Society of Mechanical Scienc-es and Engineering, 46*, Article 574. [CrossRef]

[11] Zhang, H., Zhang, L., Song, Z., & Zhu, P. (2023). Hierarchical uncertainty quantification of hybrid (riveted/bonded) single lap aluminum-CFRP joints with structural multiscale characteristic. *Composite Structures, 324*, Article 117561. [CrossRef]

[12] Haddou, Y. M., Salem, M., Amiri, A., Amiri, R., & Abid, S. (2023). Numerical analysis and optimization of adhesively-bonded single lap joints by adherend notching using a full factorial design of experiment. *International Journal of Adhesion and Adhesives, 126*, Article 103482. [CrossRef]

[13] Rangaswamy, H., Sogalad, I., Basavarajappa, S., Acharya, S., & Patel, G. C. (2020). Experimental analysis and prediction of strength of adhesive-bonded single-lap composite joints: Taguchi and artificial neural network approaches. *SN Applied Sciences, 2*, Article 1055. [CrossRef]

[14] Choudhury, M. R., & Debnath, K. (2020). Experimental analysis of tensile and compressive failure load in single-lap adhesive joint of green composites. *International Journal of Adhesion and Adhesives, 99*, Article 102557. [CrossRef]

[15] Gajewski, J., Golewski, P., & Sadowski, T. (2021). The use of neural networks in the analysis of dual adhesive single lap joints subjected to uniaxial tensile test. *Materials, 14*(2), Article 419. [CrossRef]

[16] Chen, Y., Li, M., Yang, X., & Luo, W. (2020). Damage and failure characteristics of CFRP/aluminum single lap joints designed for lightweight applications. *Thin-Walled Structures, 153*, Article 106802. [CrossRef]

[17] Silva, G. C., Beber, V. C., & Pitz, D. B. (2021). Machine learning and finite element analysis: An integrated approach for fatigue lifetime prediction of adhesively bonded joints. *Fatigue & Fracture of Engineering Materials & Structures, 44*(12), 3334–3348. [CrossRef]

[18] Bellini, C., Parodo, G., & Sorrentino, L. (2020). Effect of operating temperature on aged single lap bonded joints. *Defence Technology, 16*, 283–289.

[19] Tenreiro, A. F. G., Lopes, A. M., & da Silva, L. F. M. (2023). Damage metrics for void detection in adhesive single-lap joints. *Mathematics, 11*(4127), 1–43. [CrossRef]

[20] Park, S.-M., Roy, R., Kweon, J.-H., & Nam, Y. (2020). Strength and failure modes of surface-treated CFRP secondary bonded single-lap joints in static and fatigue tensile loading regimes. *Composites Part A, 134*, Article 105897. [CrossRef]

[21] Jensen, R. E., DeSchepper, D. C., & Flanagan, D. P. (2019). Multivariate analysis of high throughput adhesively bonded single lap joints. *International Journal of Adhesion and Adhesives, 89*, 1–10. [CrossRef]

[22] Quispe Rodríguez, R., Portilho de Paiva, W., Sollero, P., & Bertoni Rodrigues, M. R., & Lima de Albuquerque, É. (2012). Failure criteria for adhesively bonded joints. *International Journal of Adhesion and Adhesives, 37*, 26–36. [CrossRef]

[23] Goland, M., & Reissner, E. (1944). The stresses in cemented joints. *Journal of Applied Mechanics, 11*, A17–A27. [CrossRef]

[24] da Silva, L. F. M., Costa, M., Viana, G., & Campilho, R. (2017). Analytical modelling for the single-lap joint. In R. Campilho (Ed.), *Strength Prediction of Adhesively-Bonded Joints* (pp. 8–46). CRC Press. [CrossRef]